AGU PUBLICATIONS

JGR

Journal of Geophysical Research: Oceans

**RESEARCH ARTICLE**

10.1002/2016JC012087

**Key Points:**

- Gliders have been used to monitor along canyon flow, identifying upwelled cores
- Intra-seasonal reversals in the slope current have been identified in a long term ADCP record
- Variability in upwelling is associated with variability in the slope current

**Correspondence to:**
M. Porter,
marie.porter@sams.ac.uk

**Citation:**
Porter, M., M. E. Inall, J. Hopkins, M. R. Palmer, A. C. Dale, D. Aleynik, J. A. Barth, C. Mahaffey, and D. A. Smeed (2016), Glider observations of enhanced deep water upwelling at a shelf break canyon: A mechanism for cross-slope carbon and nutrient exchange, *J. Geophys. Res. Oceans*, *121*, 7575–7588, doi:10.1002/2016JC012087.

Received 23 JUN 2016
Accepted 14 SEP 2016
Accepted article online 19 SEP 2016
Published online 18 OCT 2016

# Glider observations of enhanced deep water upwelling at a shelf break canyon: A mechanism for cross-slope carbon and nutrient exchange

**M. Porter[1], M. E. Inall[1,2], J. Hopkins[3], M. R. Palmer[3], A. C. Dale[1], D. Aleynik[1], J. A. Barth[4], C. Mahaffey[5], and D. A. Smeed[6]**

[1]Scottish Association for Marine Science, Argyll, UK, [2]Department of Geosciences, Grant Institute, University of Edinburgh, Edinburgh, UK, [3]National Oceanography Centre, Liverpool, UK, [4]College of Oceanic and Atmospheric Sciences, Oregon State University, Corvallis, Oregon, USA, [5]Department of Earth, Ocean and Ecological Sciences, University of Liverpool, Liverpool, UK, [6]National Oceanography Centre, Southampton, UK

**Abstract** Using underwater gliders we have identified canyon driven upwelling across the Celtic Sea shelf-break, in the vicinity of Whittard Canyon. The presence of this upwelling appears to be tied to the direction and strength of the local slope current, which is in itself highly variable. During typical summer time equatorward flow, an unbalanced pressure gradient force and the resulting disruption of geostrophic flow can lead to upwelling along the main axis of two small shelf break canyons. As the slope current reverts to poleward flow, the upwelling stops and the remnants of the upwelled features are mixed into the local shelf water or advected away from the region. The upwelled features are identified by the presence of sub-pycnocline high salinity water on the shelf, and are upwelled from a depth of 300 m on the slope, thus providing a mechanism for the transport of nutrients across the shelf break onto the shelf.

## 1. Introduction

Globally, there are over 660 submarine canyons [*De Leo et al.*, 2010]. They incise the continental margins of all ocean basins and are known hotspots of enhanced deep-sea sediment and water flux [*Savoye et al.*, 2009], dense water cascades [*Canals et al.*, 2009], benthic biomass [*Duineveld et al.*, 2001] and fishing activity. The complex, irregular topography of the canyons can lead to internal wave generation [*Kunze et al.*, 2002], focusing of internal wave energy [*Vlasenko et al.*, 2016], enhanced diapycnal mixing [*Carter and Gregg*, 2002], and localized up and downwelling [*Allen and Durrieu de Madron*, 2009].

In shelf sea environments where the transport of nutrients and carbon between the shelf and open ocean is a crucial component of the Continental Shelf Carbon Pump [*Gruber*, 2015; *Laruelle et al.*, 2014; *Thomas et al.*, 2004; *Tsunogai et al.*, 1999] the dynamics of cross-slope flow are of particular importance. The shelf seas require a supply of nutrients to fuel their disproportionately large contribution to global primary productivity [*Simpson and Sharples*, 2012], and as a means of exporting carbon removed from the atmosphere to the deep ocean below the permanent thermocline. Due to distance from the coast, at the edges of wide shelves such as the NW European shelf this nutrient supply is largely from the open ocean [*Proctor et al.*, 2003].

The Taylor-Proudman theorem states that linear, inviscid and steady geostrophic flow will be constrained to follow f/h contours, thus inhibiting cross-slope exchange [*Brink*, 1998]. However where the assumptions of Taylor-Proudman are violated exchange is possible. The presence of narrow (narrower than the local Rossby radius) canyons can prevent currents from obeying this theorem, potentially leading to an unbalanced pressure gradient force. Depending on the direction of the incident current this may allow for up or downwelling along the axis of the canyon [*Allen and Hickey*, 2010]. On the eastern boundary of a northern hemisphere basin a poleward slope current may drive downwelling, and equatorward slope currents, upwelling. This process can allow submarine canyons on the continental margins to act as conduits between the deep oceans and the shallow seas.

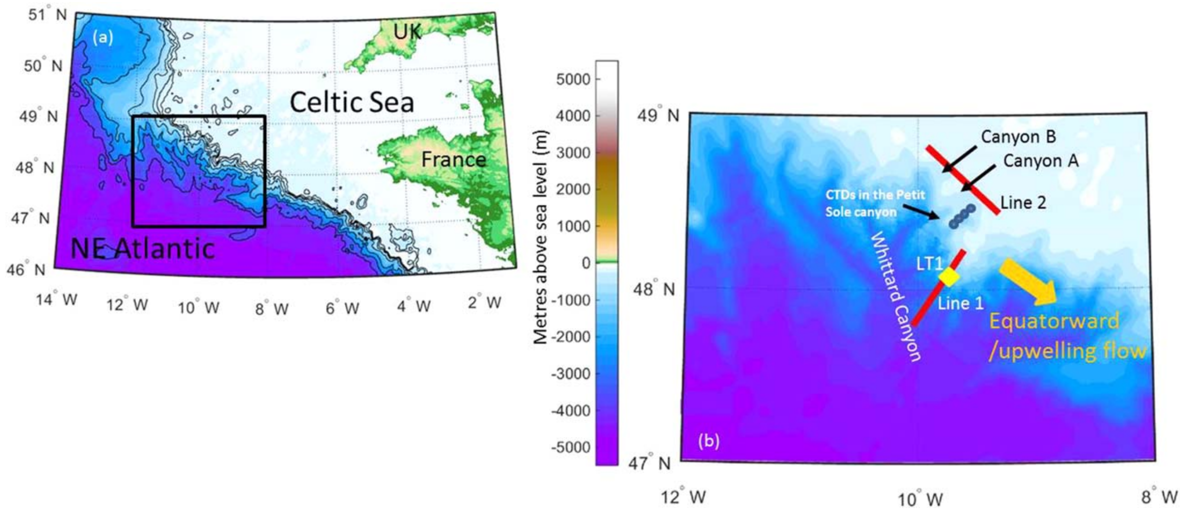

**Figure 1.** Bathymetric maps of the study region. The topography data are from Etopo1, with superimposed multibeam (GSI Dublin) data were available in Figure 1b. (a) The 200 m, 300 m, 500 m, 1000 m, 2000 m, 3000 m, and 4000 m isobaths picked out by black contours. (b) The glider transects used within this study, indicated by the red lines and the location of the ADCP mooring is shown by the yellow diamond. The canyons referred to in the text are labeled A and B. The CTD transect is shown by blue circles.

Up and downwelling through canyons, due to ageostrophic flow and the resulting ability of the current to follow the pressure gradient has been identified on shelf breaks world-wide. Examples can be seen on the west coast of North America [*Alford and MacCready*, 2014] and the west coast of Africa [*Hagen*, 2001], amongst other places. The phenomenon was first identified by *Freeland and Denman* [1982], who saw a dense pool of the water at the head of a tributary canyon of the Juan de Fuca canyon, off the west coast of Canada. Freeland and Denman's finding spurred modelling studies [e.g., *Allen and Hickey*, 2010; *Jordi* et al., 2008; *Klinck*, 1989] which when combined with subsequent observational campaigns [e.g., *Alford and MacCready*, 2014; *Alvarez et al*., 1996] have highlighted that the up/downwelling potential of a canyon is not simply a function of a large Rossby number on the downstream corner. The local stratification [*Allen and Hickey*, 2010], the incident current [*Allen and Hickey*, 2010] and the canyon geometry [*Allen and Hickey*, 2010; *Allen*, 2000] also have an impact on the direction and intensity of along canyon-axis flow. Further observational studies have shown that canyons with up/downwelling currents rarely experience either of them as persistent features, with both upwelling and downwelling being seen in a given canyon [*Allen and Durrieu de Madron*, 2009]. Furthermore the occurrences of up/downwelling events in canyons have been observed to be sporadic [*Freeland and Denman*, 1982].

To further the understanding of seasonal flow dynamics around shelf edge canyons and the role they play in ocean-shelf exchange it is necessary to develop methods that can be used for canyons along the edges of broad shelves and during rough conditions.

In the North East Atlantic the Celtic Sea slope is a noncoastal, continental margin environment. The shelf is wide (circa 300 km) and its slope is a region of highly complex topography, where over 30 canyons incise a 300 km stretch of the shelf edge between the Celtic and Armorican margins [*Bourillet et al*., 2003]. Along the slope is a predominantly poleward slope current, driven largely by the joint effect of baroclinicity and bottom relief (JEBAR) [*Huthnance*, 1984] and constrained to follow the topography by Taylor-Proudman theorem. In addition to the JEBAR effect this slope current follows SOMA (September/October–March/April) variability [*Pingree and Le Cann*, 1989; *White*, 2003; *Xu et al*., 2015]. During the winter months strong prevailing south-westerly winds combined with a meridional density gradient gives a poleward slope current [*Huthnance*, 1984]. However in the summer, relaxing of the south-westerly winds and variability in sea surface height leads to a reversal [*Pingree and Le Cann*, 1989; *Porter et al*., 2016].

Within this study we focus on Whittard Canyon, a large canyon (width of ~55 km at the 2000 m contour) on the Celtic Sea slope that is part of the Canyon Marine Conservation Zone [*JNCC*, 2013] with a complicated series of tributary canyons incising the shelf (Figure 1). The main channel is deep, largely oriented in an along-shelf direction and wide when compared to the local first baroclinic Rossby radius of deformation ($L_R$)

($L_R = \sqrt{(g' \times D)}/f$ where D is the pycnocline depth and $g' = g\,(\rho_1 - \rho_2)/\rho$ where $g = 9.81\ ms^{-2}$, $\rho_1$ the density of the upper (above pycnocline) water, $\rho_2$ the density of the lower (below pycnocline) water and $\rho$ the mean density, here $L_R \approx 12$ km. This large ratio of channel width to $L_R$ allows the flow to stay in geostrophic balance and thus not flow down the pressure gradient. However, a number of the smaller tributary canyons cut across the slope approximately perpendicular to both the slope and the geostrophic slope current. Two of these canyons (A and B on Figure 1) drop from a depth of 200 m at the shelf-break to 3500 m in the bottom of Whittard canyon, over a distance of approximately 5 km. They are narrow, approximately 6–7 km at their 1000 m depth contour, and are approximately half of the local $L_R$.

Along the European shelf break the presence of the slope current can be sufficient to cause cross-slope exchange through Ekman veering of near bed currents, which similarly to canyon related geostrophic imbalance can help to move water on shelf during equatorward flow and off shelf during poleward flow [*Kundu*, 1976; *Huthnance et al*., 2009; *Simpson and McCandliss*, 2013]. At the Celtic Sea slope the interaction of the barotropic tide with the irregular and steep (super-critical) slope creates a region of high internal wave activity during the stratified, summer months [*Huthnance et al*., 2001]. Previously it has been shown that cross-slope exchange in this region is dominated through processes related to internal waves, which can be nonlinear and propagate from the shelf-break across the shelf toward the coast, transporting mass and energy [*Green et al*., 2008; *Inall et al*., 2011]. The internal wave energy and the resultant mixing along the shelf break is locally focused in the canyons along this slope [*Vlasenko et al*., 2016]. Furthermore, intense mixing at the shelf break, due to internal waves, is also thought to lead to the exchange phenomenon of "salt lenses," which transport high salinity water over 100 km onto the shelf [*Hopkins et al*., 2012]. During winter, heat loss from the ocean to the atmosphere leads to convective mixing which breaks down surface stratification and ultimately erodes the seasonal thermocline. Consequently the previously described processes, which rely on a stratified environment are diminished or eliminated. The persistence of the slope current year round creates an environment conducive to cross-slope exchange through canyon driven up and downwelling, in addition to Ekman veering beneath the slope current. However, the direct importance of canyons on the Celtic Sea slope as a conduit for cross-shelf exchange has not previously been studied.

Since 2001 the introduction of underwater gliders for hydrographic surveys has allowed us to remotely capture high resolution, spatiotemporal representations of underwater regions [*Rudnick et al*., 2004]. Gliders do not necessarily require the presence of a large ship and they can remain in the water for up to 6 months. The semi-autonomous nature of the gliders and their relative low cost allows for repeated campaigns, giving us easier access to hydrographic data during the winter and in remote regions. Additionally they allow for reactive adaptations in the sampling strategy, producing observational data sets that are highly targeted to a specific objective.

In this study we show the use of gliders around subsurface, shelf break canyons, highlighting gliders as a data collection instrument that may allow us to ascertain the importance and impact of these canyons on a year round and global basis. We use a moored current profiler to show the seasonality of the slope current on the Celtic Sea slope, indicating that both up and downwelling scenarios are possible. During summer time equatorward flow localized upwelling hotspots are identified, which show a clear decline as the slope current reverses.

The remainder of the paper is structured as follows: In section 2, we introduce the data and methods that have been used to provide a spatio-temporal understanding of the hydrographic structure near to two submarine canyons on the Celtic slope. The results of this are then presented in section 3 followed by a discussion of variability as well as its further impact on nutrient and carbon exchange and the final conclusions in section 4.

## 2. Methods and Data

Within this study two Slocum Gliders [*Jones et al*., 2005] were flown as a pair, one perpendicular to the shelf break, across the slope (Line 1, Figure 1), and the other parallel to the shelf break (Line 2, Figure 1), (Table 1). The gliders remained in this paired configuration, collecting CTD data for 23 days between the 24 July and the 15 August 2012, with the occupation of Line 1 continuing then through until January 2013. This formation allowed us to observe the properties of the water flowing over the canyons, perpendicular to their main axis, and simultaneously the water shelf-ward of the canyons, parallel with their main axis (Figure 1).

**Table 1.** The Instruments and Sensors Used Within This Study Their Locations (With Reference to Figure 1) and Their Dates of Deployment (Indicated by the Black Bars Within the Table)

| Instrument | Sensor | Occupation location | 2012 | | | | | | | 2013 | | | |
|---|---|---|---|---|---|---|---|---|---|---|---|---|---|
| | | (referencing Figure 1) | June | July | August | September | October | November | December | January | February | March | April |
| Slocum glider (SN 330) | CTD - SBE 41 | Line 1 | □□□■ | ■■■■ | ■■■□ | □□□□ | □□□□ | □□□□ | □□□□ | □□□□ | □□□□ | □□□□ | □□□□ |
| Slocum glider (SN 194) | CTD - SBE 41 | Line 2 | □□□□ | □□■■ | ■■□□ | □□□□ | □□□□ | □□□□ | □□□□ | □□□□ | □□□□ | □□□□ | □□□□ |
| Seaglider (sg156) | CTD - SBE-3 and SBE-4 | Line 1 | □□□□ | □□□□ | □□□□ | □□□■ | ■■■■ | ■■■■ | ■■■■ | ■■■■ | □□□□ | □□□□ | □□□□ |
| ADCP | 75kHz RDI ADCP and 75kHz Flowquest ADCP | LT1 | □□□□ | ■■■■ | ■■■■ | ■■■■ | ■■■■ | ■■■■ | ■■■■ | ■■■■ | ■■■■ | ■■■■ | ■■■■ |
| CTD rosette | SBE-3 and SBE-4 | PS canyon | □□□■ | □□□□ | □□□□ | □□□□ | □□□□ | □□□□ | □□□□ | □□□□ | □□□□ | □□□□ | □□□□ |

During the 23 days of the canyon-focused glider campaign the gliders collected 248 CTD profiles on Line 1 across the slope and 282 on Line 2 along the shelf, using unpumped SeaBird Electronics CTD sensors (SBE 41). The salinity data collected by these gliders have been cross calibrated with a CTD on the LT1 mooring (yellow diamond in Figure 1) and each other, where appropriate. These data comparisons suggested that there was no sensor drift over the period of this experiment. The calibrated data have been corrected for errors arising from flow speed through the sensors and temperature lag due to thermal inertia within the conductivity cell following the methods of *Garau et al*. [2011]. Each transect was translated onto a 5 km x 5 m grid. Subsequently these grids were interpolated using a Barnes' optimal analysis method [*Barnes*, 1994], using a horizontal interpolation radius of 15 km, reflecting the autocorrelation of the data and the local internal Rossby radius.

The Celtic Sea slope is subject to strong, nonlinear internal tides [*Green et al*., 2008; *Vlasenko et al*., 2014]. As each glider samples through both time and space it is necessary to mitigate the effects of subsampling or aliasing these internal tides, or at least to be aware of their presence when interpreting the data. In order to most clearly visualize the data and to limit the impact of the internal tide as well as ensuring full data coverage, the transects have been averaged into time means. It is made clear throughout this paper whether the transect being referred to is a single pass or a time mean and over what period averaging has been applied.

In order to contextualize any up/downwelling identified within the canyons it is necessary to know the strength and direction of the local slope current. The velocity structure of the slope current, adjacent to the glider sections, was measured throughout this campaign by two moored 75 kHz long range ADCPs on mooring LT1 (Figure 1 and Table 1). The ADCP time series have been filtered using a 71 h Godin filter, removing the tides. A section of the water column, between 500 m and 1000 m, assumed to be in geostrophic balance, had a mean flow with a bearing of 302°. A clockwise rotation of 58° is therefore applied such that v velocity is aligned locally along the slope (positive poleward) and u locally aligned across-shelf (positive on-shelf).

Through CTD and nutrient profiles in the Petit Sole Canyon (Figure 1) we are able to understand the impact that through canyon upwelling may have on local nutrient exchanges. On these profiles inorganic nutrient concentrations were determined using a Bran and Luebbe QuAAtro five-channel segmented flow nutrient analyzer using standard colorimetric techniques [*Grasshoff et al*., 2009]. Unfiltered seawater samples collected directly from the Niskin bottle were analyzed onboard for concentrations of nitrate plus nitrite (N+N], phosphate (P) and silicate (Si). The limits of detection for N+N, P and Si were 0.1, 0.05 and 0.1 $\mu$M and precision was better than 1%.

We will return to the nutrient data in the discussion. First, we will look at the data collected by the gliders on Lines 1 and 2, and the ADCP at LT1.

## 3. Results

Between the 24 July and the 15 August 2012 the depth average current between 500 m and 1000 m at LT1 showed the slope current to be dominated, as expected, by the along-slope component (Figure 2b). Within this variability, patterns can be identified which show equatorward flow until the 3 August, followed by poleward flow until the 13 (Figure 2a).

Next we discuss the glider transects, averaged over the full 23 day campaign and split between the poleward and equatorward phases of the slope current as identified at LT1 (Figure 2a).

### 3.1. Across-Slope Hydrography (Line 1)

During this 23 day study the glider on Line 1 completed five transects, which have been averaged to give a campaign-long overview of the hydrographic structure on this line (Figures 3a and 3b).

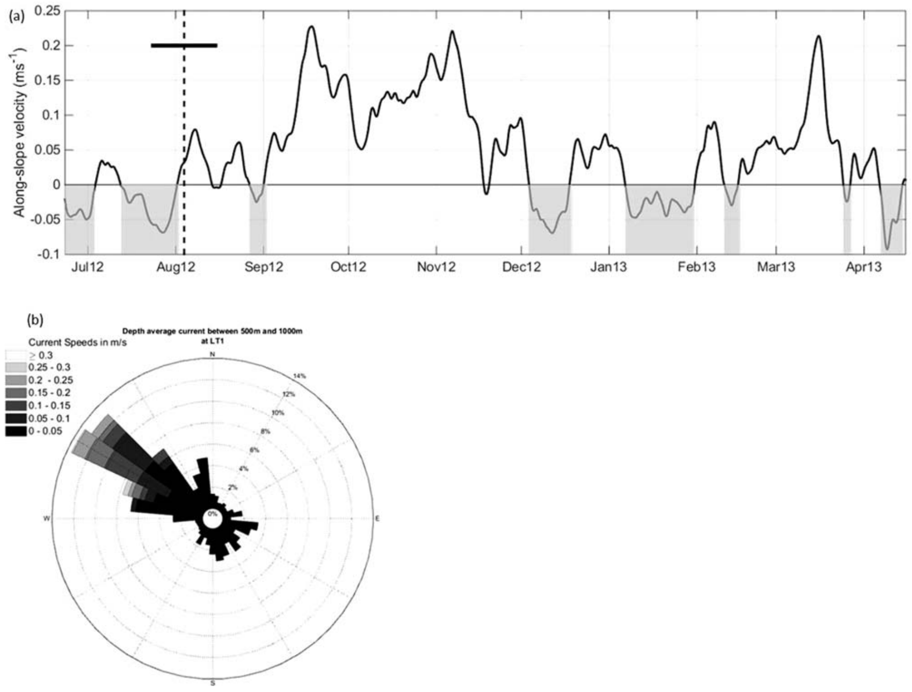

**Figure 2.** (a) The along-slope component velocity of the depth average from 500 to 1000 m from the ADCP at LT1. Poleward flow is signified by positive velocity and equatorward by negative. The dashed black line shows 5 August, the short, solid black line indicates the glider canyon campaign and the dashed orange boxes highlight equatorward flow. (b) The directions (angle) and frequency (spoke length) as well as the speed (shading) of the 500 m – 1000 m depth average current at LT1. This current rose covers that same period as Figure 2a.

We begin by looking at the density structure on the time mean transect. Across the transect the mean pycnocline depth varied between 20 m and 60 m, indicative of summer stratification and a shallow surface mixed layer. Stable stratification throughout the remainder of the water column (mean buoyancy frequency, N = 0.0041 rad s$^{-2}$) appears to mask the variability in the salinity structure. The large range in temperature compared to that of salinity (Figures 3a and 3b) gives a temperature dominated stratification profile, allowing salinity to act as a tracer of different water masses.

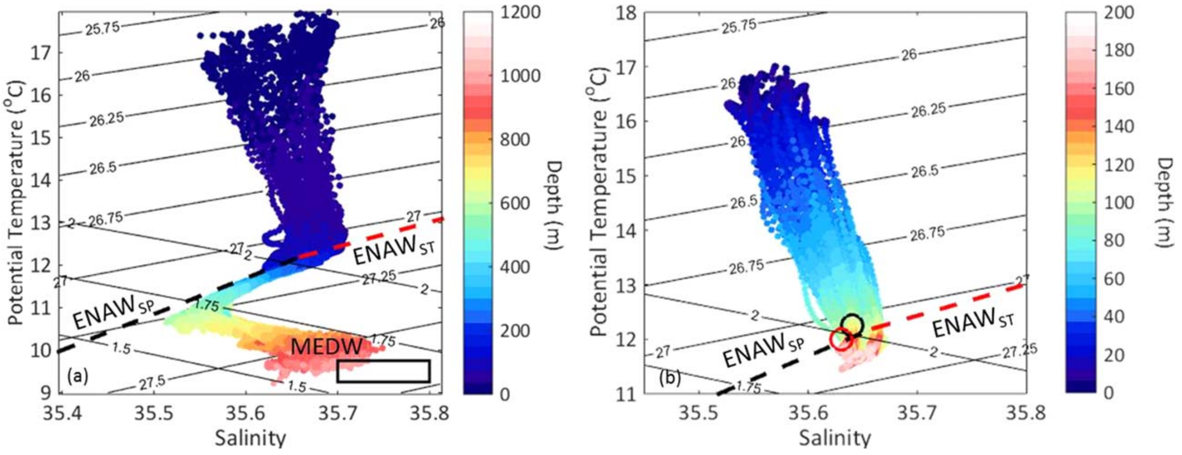

**Figure 3.** (a and b) Line 1 (across slope) and show the time mean transects between 24 July and 15 August from glider 330, (c and d) Same time means from Line 2 (along slope), using glider 194. (a and c) Salinity, (b and d) temperature. The black contours indicate the density.

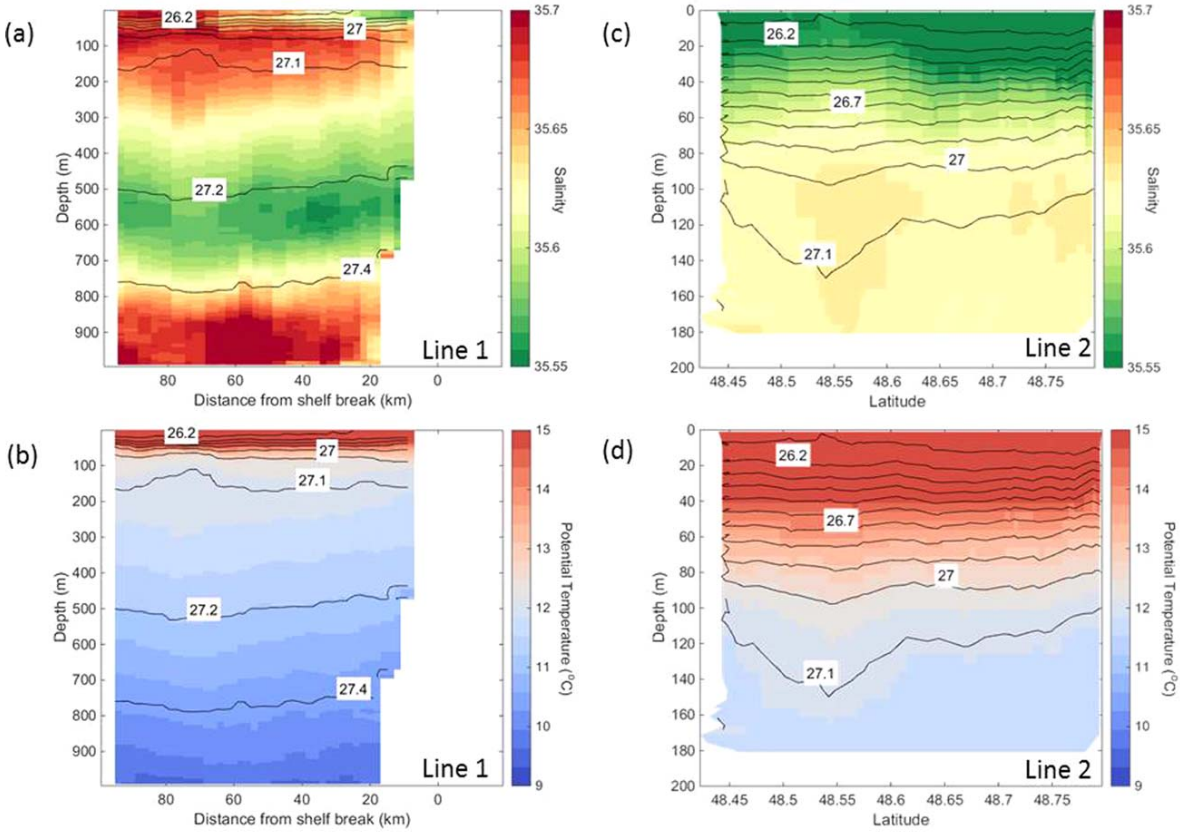

**Figure 4.** Potential temperature and salinity plots for all profiles on (a) line 1 and (b) line 2. The plots are coloured by depth, it should be noted that the colorbar scale is different on each plot. The red dashed line shows the properties of the $ENAW_{ST}$, the black dashed line, $ENAW_{SP}$ and the black box MEDW (acronyms defined in text). The contours sloping up toward the right of the plot show potential density and down to the right of the plot show selected spice levels. In Figure 4b, the two circles highlight water sourced on the shelf (red) and within the salinity cores (black) at 110 m depth, during equatorward slope current flow.

The time mean temperature and salinity transects show a three-layer salinity structure (Figure 3a), highlighted in the potential temperature-salinity plot (Figure 4a). The transects are dominated by the presence of Eastern North Atlantic Water (ENAW, practical salinity (S) = 35.23–36.12 potential temperature ($\Theta$) = 8.56–14.86°C [*Pollard et al.*, 1996]), which sits below the seasonal pycnocline at ~100 m to a depth of approximately 700 m. The upper 100 m of this layer contains a tongue of water of subtropical origin ($ENAW_{ST}$ $S>35.62$ $\Theta = 12.2$ - 14.86°C [*Pollard et al.*, 1996]), whereas the remainder is cooler, fresher and of subpolar origin ($ENAW_{SP}$). While the shallow tongue of $ENAW_{ST}$ is largely isobaric across the transect the deeper $ENAW_{SP}$ upwells toward the slope. Below the ENAW, in the deepest part of the glider section, the upper limit of Mediterranean Water (MEDW, $S>35.7$ $\Theta\sim9.5$°C [*Harvey*, 1982]) can be identified by a deep salinity maximum.

### 3.2. Along-Shelf Hydrography (Line 2)

Throughout the same 23 day period, six transects were made along Line 2. Line 2 sampled perpendicular to the main axis and near to the head of two cross-slope tributary canyons within Whittard Canyon (A and B in Figure 1). Similar to Line 1, the stable stratification ($N = 0.076$ rad $s^{-2}$) and small environmental range of salinity on Line 2 indicate that temperature dominates the density field. The main features are again most clearly identified by salinity contours. (Figure 3c)

The time mean transect of salinity on Line 2 shows the pycnocline at a depth of approximately 80 m, with mixed layer salinity ranging from 35.53 at the surface to 35.62 at around 80 m (Figure 3c). Below the pycnocline the salinity remains largely homogeneous to the bottom, with the exception of two cores of more saline water ($S > 35.635$). These cores are notably located at the head of the two tributary canyons and

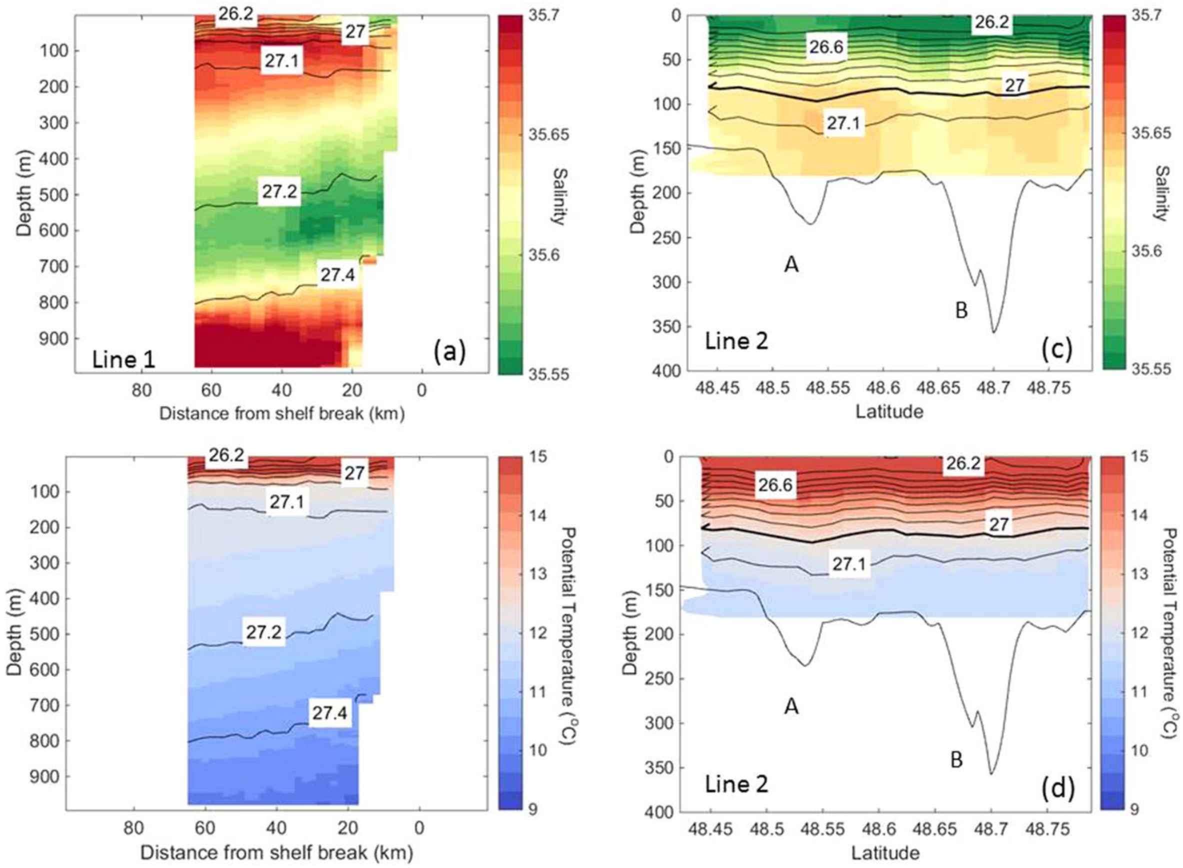

**Figure 5.** Time mean transects between 24 July and 5 August, during which time the slope current was equatorward. The transects are from (a, b) line 1 and glider 330 and(c, d) line 2 and glider 194. (a and c) Salinity, (b and d) temperature. The black contours indicate the density. The lowest line on each plot (Figure 5c and 5d) is the bathymetry at the shelf-break, with the canyons A and B (Figure 1) labeled.

appear to show ingress of ENAW onto the shelf (Figures 3c, 3d, and 4b), suggesting that the canyons may experience upwelling.

In order to further investigate these salinity cores and the potential for canyon enhanced upwelling in this region we have split the data before and after the 4 August to represent hydrographic conditions when the depth mean flow according to the ADCP data was equatorward (upwelling favorable) and when it is poleward (downwelling favorable). During each of these periods the tidal phase was similar, with each up/downwelling favorable phase comprising parts of both the spring and neap tide. Consequently it has been assumed that the results observed are not due to spring-neap differences. The glider transects throughout these two periods will be discussed next.

### 3.3. Equatorward Slope Current

Prior to and during the first half of this campaign, up until the 4 August 2012 the ADCP at LT1 showed that for 29 of the 39 days the water column between 500 m and 1000 m flowed, on average, along the slope toward the equator (Figure 2). The three Line 1 and three Line 2 transects carried out prior to the 4 August (24 July to 5 August) have been averaged, creating one time mean transect for the shelf (Line 1) and one for the slope (Line 2) representing upwelling favorable conditions. These transects show similar structure to the full experiment means, with a three-layer salinity structure on the slope and two high salinity cores on an otherwise stratified shelf (Figure 5). The presence of 2 salinity cores at the head of the canyons is largely consistent throughout each of the transects averaged within this mean (Figure 6).

Comparison of the water properties in the high salinity cores on Line 2 with the water on Line 1 indicates that the water within the high salinity cores was upwelled from a layer with the same temperature and salinity

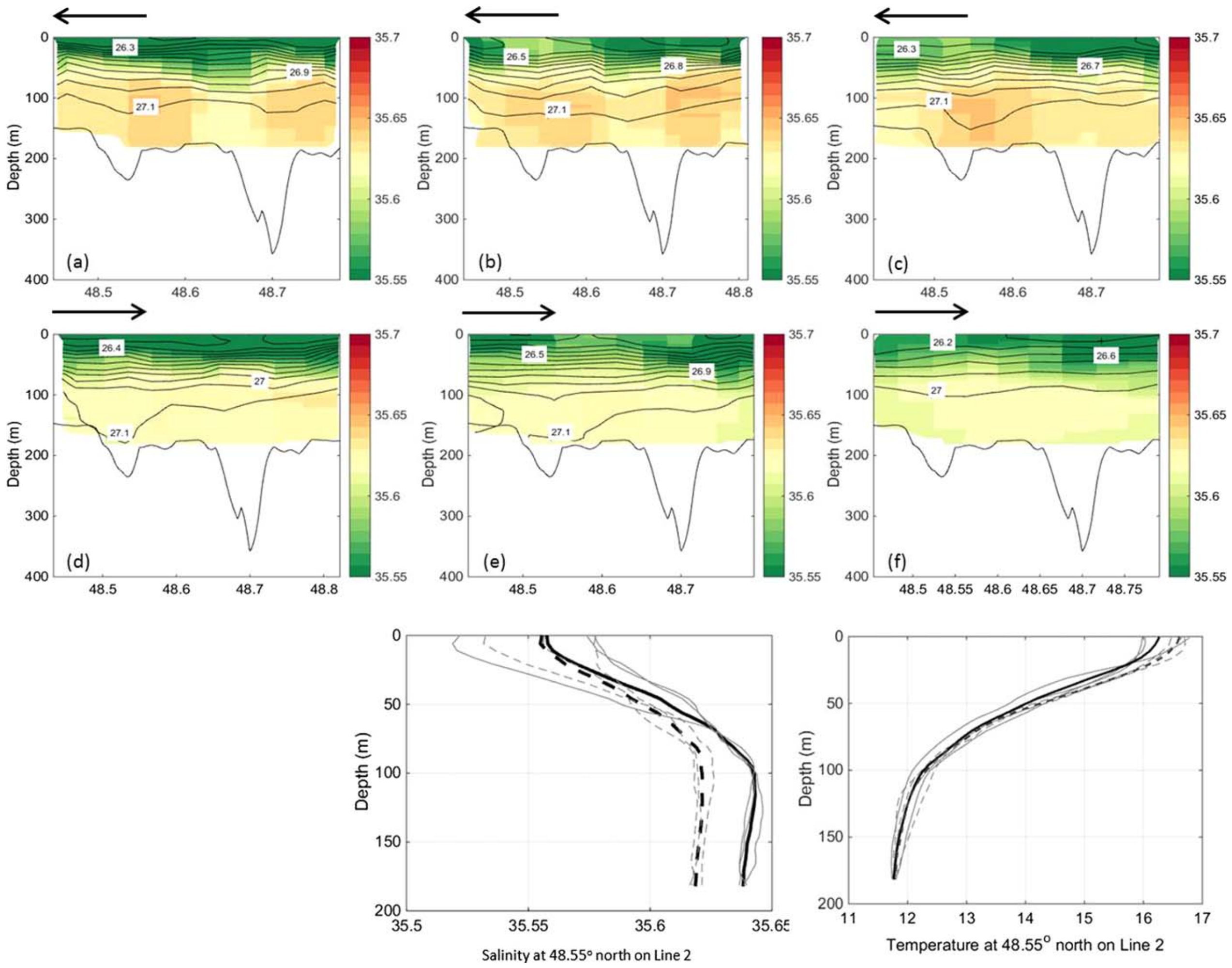

**Figure 6.** The individual salinity transects along line 2, from (a–f) glider 194, (g) the salinity profiles and (h) temperature profiles through each of these at 48.55°. The (g, h) solid lines indicate (a, c) transects and (d, e) the dashed, the heavy lines show the mean profiles. The arrow above each plot shows the relevant slope current direction.

properties as the water between 150 m and 300 m depth on Line 1 (Figure 5). This estimate is in agreement with the scaling analysis for upwelling depth below shelf break (Z), derived by *Allen and Hickey* [2010];

$$Z=1.4\frac{U}{N}\left(\frac{L}{R}\right)^{\frac{1}{2}} \tag{1}$$

where L is the on-shelf deviation of the 200 m isobath in the canyon, 15 km, R is the upstream radius of curvature for the 200 m isobath at the canyon mouth, 3 km, N is the buoyancy frequency (defined previously) and U is the incoming velocity (approximated here by the along slope velocity). Here Z predicts that upwelling starts 100 m below the shelf break depth, which is locally 200 m, giving an upwelling depth of up to 300 m. Alternatively we can compare the depths of isopycnals across the two transects, to infer the upwelling depth. The deepest isopycnal on line 2 is 27.1 kgm$^{-3}$, which occurs at approximately 200 m (Figure 5). This suggests a shallower upwelling depth than the scaling analysis predicts, however as the lines are not collocated the relative densities are influenced by the effects of mixing during advection. Given the advantages of using the scaling analysis to estimate winter upwelling, when isopycnal comparison is not available we have chosen to continue to use the 300 m upwelling depth, estimated by the scaling analysis.

In this environment the dominance of temperature in the density profiles allows us to use salinity variability along an isopycnal to represent spice, the quantification of temperature and salinity variability along

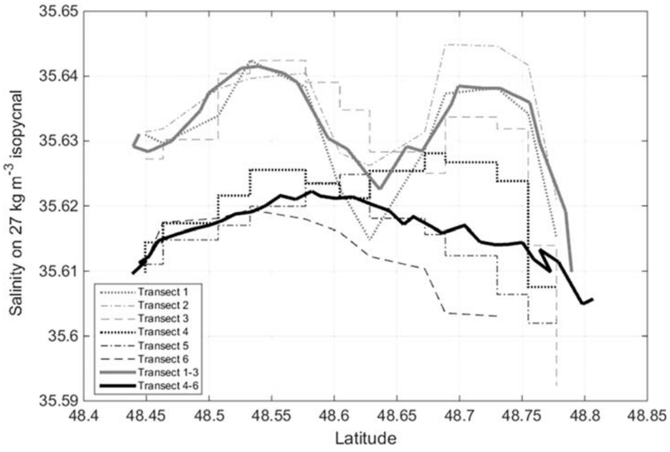

**Figure 7.** The salinity along the 1027 kgm$^{-3}$ isopycnal on transect 2 during an equatorward slope current (grey lines) and a poleward slope current (black lines). The individual transects are shown by the dotted lines (in the appropriate color for the slope current direction) and the mean transects for each slope current direction are shown by the heavy, solid lines This isopycnal is highlighted by the heavy black contour in Figures 5d, 5e, 5f, 8d, 8e, and 8f.

isopycnals [*Munk*, 1981] in order to infer local mixing and advection regimes. At the edges of the potentially upwelled salinity cores identified above, there are strong along isopycnal salinity gradients (Figure 7). These strong gradients in along isopycnal salinity and therefore implied spice have been used as indicative of the presence of strong fronts and therefore advection as opposed to local mixing [*Cole and Rudnick*, 2012; *Klymak et al*., 2015], providing further evidence that these salinity cores are upwelled slope water on the shelf.

### 3.4. Poleward Slope Current

From the 5 August until mid-November the water column between 500 m and 1000 m depth flowed, on average poleward along the slope (Figure 2). During the period in which the gliders were in the water (5 August to 15 August) the depth averaged current was in a transition phase and was weaker than later in the year. The four slope and three shelf transects carried out between these dates have been collated creating one time mean transect for Line 2 (on the shelf) and one for Line 1 (on the slope) representing un-favorable upwelling but potentially downwelling favorable conditions (Figure 8). The salinity structure on Line 1 remains similar to the campaign mean, however across Line 2 only vague remnants of the salinity cores can be seen. This transect is also notably fresher than during equatorward flow, with a mean sub-pycnocline salinity of 35.61.

The time mean transect shows that over Canyon A (Figure 1) there was localized high temperature without a concurrent salinity signal (Figure 8). The resulting increase in isopycnal thickness (Figure 8) and simultaneous reduction in along isopycnal salinity gradient (Figure 7) indicates no local fronts, suggesting that that this is a mixed environment [*Cole and Rudnick*, 2012]. However, we cannot discount advection of the salinity cores onshelf through onshelf currents or offshelf due to through canyon downwelling. This termination of the upwelling system is corroborated by the T-S plot which suggests that the water on the slope and the shelf is distinct during this time (Figure 4).

Individual transects give further detail on the termination of the upwelling (Figure 6); the first transect completed under poleward current conditions has notably higher sub-pycnocline salinity than the following transects (Figure 6d). With each pass of the gliders the water freshens, suggesting that any remnants of the high salinity cores are being removed from the local environment by advection on shelf, entrainment into downwelling or through mixing and are no longer being supplied with high salinity water. Significantly, on Line 1 the hydrographic structure in the shelf break region remained similar throughout the survey, thus the changes seen on the slope do not simply reflect changes in the off-shelf water. The lack of an identifiable salinity core in the first transect under a poleward slope current indicated that the upwelling ceased soon after the reversal in the slope current. This supports the hypothesis that during a poleward slope current there is no upwelling through the canyons, although we do not have the data to ascertain whether a period of downwelling is apparent under these conditions.

Using 2 gliders working perpendicular and parallel to the shelf break in association with a mooring mounted ADCP we have shown that canyons in the Celtic Sea slope cause oceanic water to cross onto the shelf. We see observational evidence that during equatorward flow of the slope current upwelling through the canyons is from the theoretical upwelling depth of 300m. We suggest that under these conditions the canyons can disrupt geostrophic flow and allow water to follow the pressure gradient force onto the shelf.

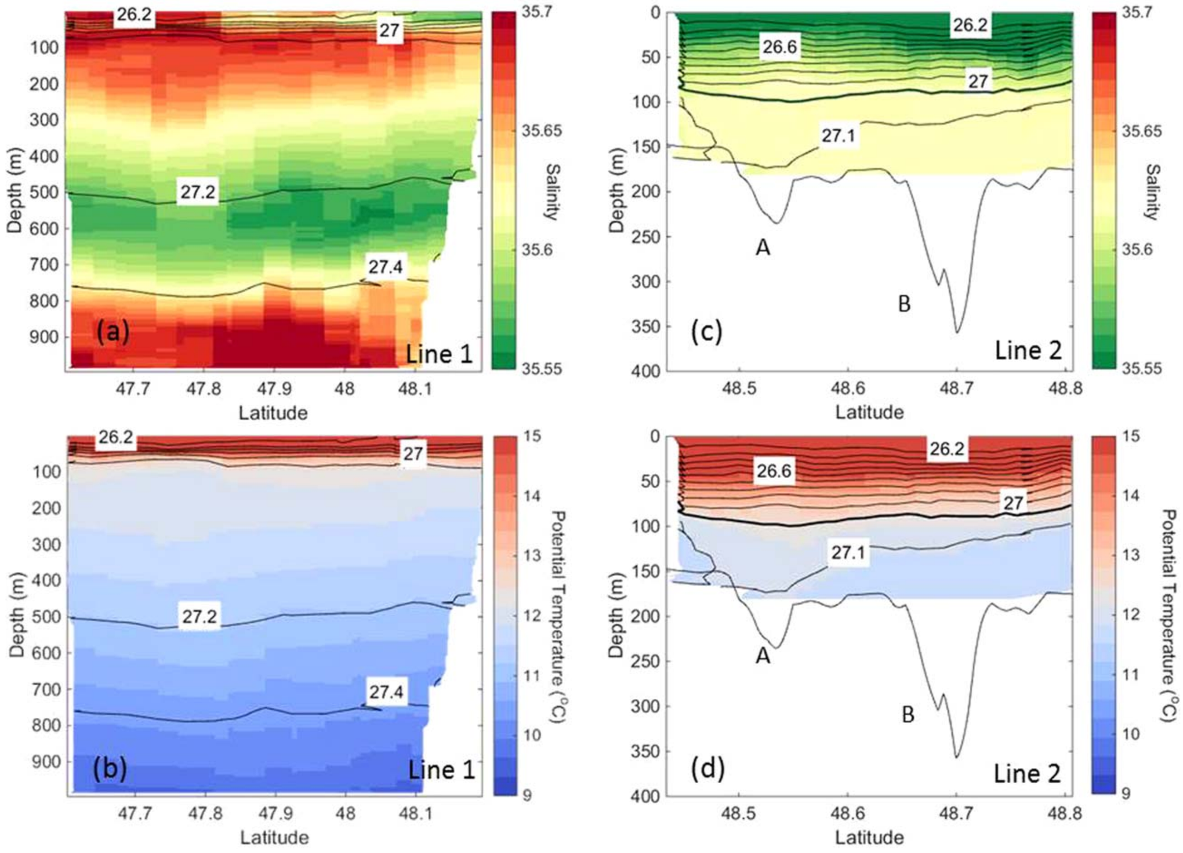

**Figure 8.** Time mean transects between 5 August and 15 August, during which time the slope current was poleward. The transects are from (a, b) transect 1 and glider 330 and(c, d) transect 2 and glider 194. (a, c) Salinity, (b, d) temperature. (c–e) The black contours indicate the density and the lowest line on each plot is the bathymetry at the shelf-break, with the canyons A and B (Figure 1) labeled.

## 4. Discussion and Summary

### 4.1. Variability

Hydrographic glider surveys continuing throughout 2012 on Line 1 combined with continued measurements at LT1 have allowed the variability around the upwelling within these canyons to be assessed.

The switch in the direction of the slope current (depth average of 500 m to 1000 m at LT1) from predominantly equatorward to predominantly poleward reflects the continued variability. The poleward flow, which began in August largely persisted until December 2012, after which time the flow was dominated poleward flow but frequently saw equatorward reversals (5 between the start of December and mid-April). We suggest that this is poleward dominated winter flow is consistent with the well documented SOMA (September/October–March/April) effect [*Pingree and Le Cann*, 1989; *White*, 2003; *Xu et al.*, 2015]. In conjunction with the observations from this study the SOMA variability indicates that the ability of the canyons to act as conduits between the slope and the shelf is likely to be largely seasonal.

While the data collected here do not allow for the identification of downwelling within the canyon, previous canyon flow studies indicate that this process is likely, but that it is also likely to be weaker than the equivalent upwelling [*Allen and Durrieu de Madron*, 2009]. The seasonality of flow within the canyons may therefore play a role in the continental slope Carbon Pump. When an equatorward slope current occurs in early spring, prior to the spring bloom, upwelling through the canyons may provide deep, nutrient rich water to the shelf. Subsequently, after spring/summer production, the occurrence of a poleward slope current may help to drain the dissolved inorganic carbon (DIC) rich shelf water into the deeper ocean. This potential up

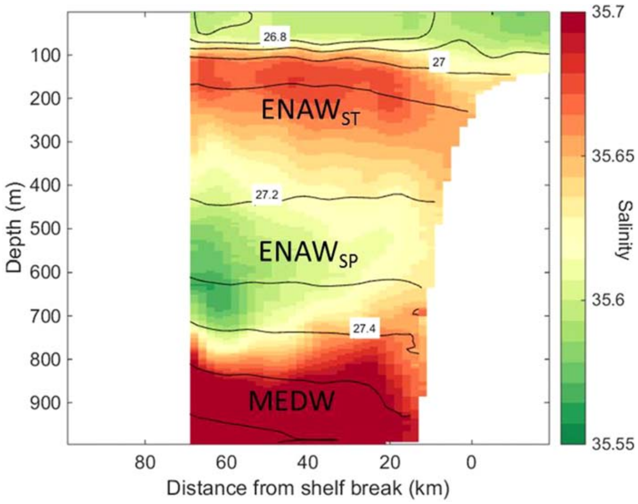

**Figure 9.** The time mean salinity on line 1 averaged between the 31 October 2012 and the 28 November 2012. The contours show potential density

and downwelling through the canyons, though asymmetrical, would provide a seasonal rectifier, pumping nutrients onto the shelf in the early summer and pumping DIC off the shelf in autumn and winter.

It is clear throughout the ADCP time series that small scale variability in slope current direction, atypical for the specific SOMA season is frequent (Figure 2). During the record there are 8 periods of equatorward flow lasting between 3 and 24 days which have the potential to drive through canyon upwelling. Consequently, intermittent upwelling may also be important during the winter, when the hydrographic properties of the water impacting the canyons are different to during the observed, summer period. In early December when the prevailing poleward slope current was briefly interrupted by equatorward flow during which time one glider, SG156 (Table 1) was sampling on Line 1. Throughout this period the upwelling depth predicted by equation (1) had deepened slightly to 320 m. Glider transects during this time suggest that the water at the depth had increased in salinity (Figure 9). At the estimated upwelling depth there is an increased incidence of ENAW$_{ST}$ and consequently a change in the dominant upwelled water mass when compared to the transects studied in detail within this study.

Not only is the slope current seasonally variable, but it has notable variability in both its strength and direction on an inter-annual basis. It has previously been shown that it is possible to estimate the range in the velocity of the slope current using altimetry data [*Xu et al*., 2015] without using direct measurements. *Xu et al*. [2015] showed that altimetry derived geostrophic currents along the European slope can explain over 50% of the variability of the currents observed within ADCPs and lagrangian floats. The clear variability seen within this altimetry study indicates that on the Celtic Sea it is necessary to at least estimate the state of the slope current before inferring upwelling favorable conditions.

### 4.2. Impact on Nutrient Flux

The onset of an equatorward slope current in March/April will often precede the spring bloom of phytoplankton on the shelf [*Rees et al*., 1999]. The occurrence of canyon based upwelling associated with the slope current provides a mechanism of cross slope flow, and therefore a pathway for nutrient advection onto the shelf, during a time when a cross slope flow may otherwise be largely absent [*Hydes et al*., 2001].

On the 24 June 2012, a transect of 4 CTD profiles (Figure 1) was sampled for nutrients along the axis of the Petite Sole canyon [*Vlasenko et al*., 2016] adjacent to the canyons A and B in this study. Linear regressions suggested that the variance of the profiles of nitrate + nitrite (N+N), silicate (Si) and phosphate (P) was well explained by the potential density with mean $R^2$ of 0.96 for N+N, 0.82 for Si and 0.91 for P ($p<0.001$ for all three regressions). Assuming this relationship between density and the nutrient concentration is consistent between the 3 adjacent canyons we can use this to infer chemical properties of the upwelled water.

While Figure 6 suggests that the density may be largely temperature compensated, it is clear that there is variability in the density structure associated with the cooler and high salinity upwelled salinity cores. During upwelling favorable conditions the sub-pycnocline water is approximately 0.1 kg $m^{-3}$ denser than otherwise (Figure 10a). Given the density-nutrient relationship seen in the Petite Sole canyon this would imply that water with elevated N+N (as well as Si and P, which are not shown) has been advected onto the shelf (Figure 10a), with an increase of up to 2 $\mu$M of N+N. Correspondingly we can see that at C4 (48.4°N, 9.6°W), the deepest nutrient station, the N+N concentrations are higher at 300 m, the maximum extent of the upwelling, than at the bottom depths of the shelf station (Figure 10b).

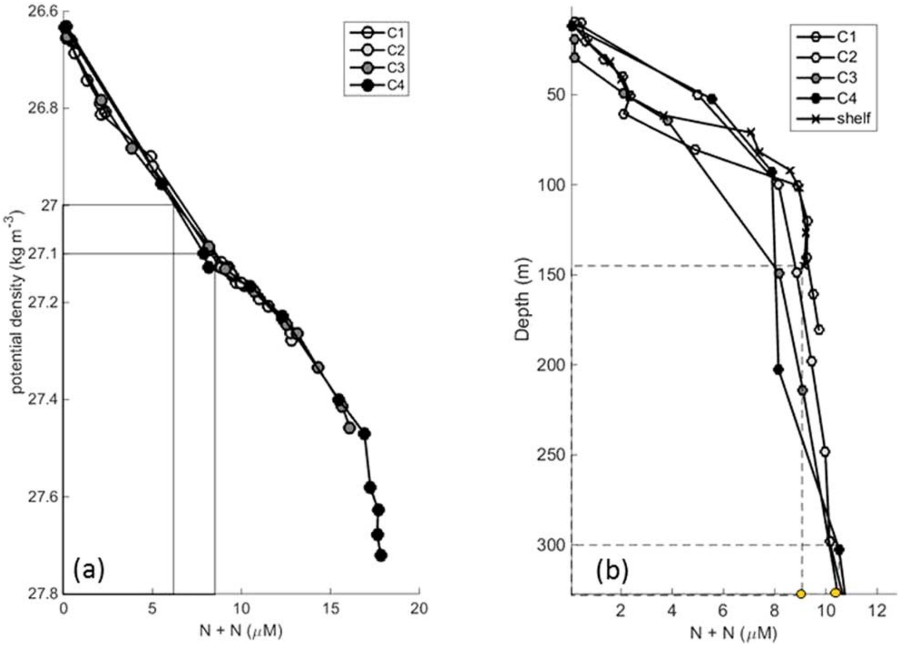

**Figure 10.** (a) Potential density profiles of Nitrate + Nitrite at 4 points along the Petite Sole canyon (C1:C4, where C1 is on the shelf and C4 at the mouth of the canyon). The solid lines indicate the background shelf density (27 kg m$^{-3}$) and the density within the salinity cores (27.1 kg m$^{-3}$), with N+N values recorded from the mid point of the 4 profiles. (b) Nitrate + Nitrate at the same 4 points in the canyon and on the shelf, shelfward of the canyon (shelf). The dashed line indicate the maximum upwelling depth and the depth of the center of the salinity cores, the yellow dots show where the C4 and shelf profiles intersect the *y* axis.

This process is likely to persist throughout the summer, adding to the pathways for nutrients onto the shelf during a period when nutrient concentrations are depleted in surface waters due to biological consumption. Subsequently, potential downwelling which may be predominant in the autumn and winter would provide a pathway to remove DIC contained in the shelf water to the deeper ocean, after the summer bloom. Throughout this period, intermittent upwelling may provide winter time nutrient pathways.

### 4.3. Summary

In this paper we have used hydrographic data from 2 gliders on the Celtic Sea slope, with further context provided by a slope based, moored ADCP. We have demonstrated that in typically summer time conditions, where the slope current is equatorward, canyons in the slope can work as a pathway for upwelling of nutrient enriched slope water onto the shelf. Conversely in typically winter time conditions, a poleward slope current, the upwelling is no longer seen.

The hydrographic surveys presented here add to the current body of work focusing on canyon driven upwelling. We have highlighted that short-term (order of 1 week) yet sustained changes in the direction of the currents incident on the canyon can drive or prevent this type of upwelling. It is clear that the gliders used within this study allow for a detailed description of the variability in these flows without the need for large and inherently expensive ship-based observational campaigns.

The seasonal reversal in the slope current, the SOMA effect, which leads to the seasonality of the upwelling is in itself variable on a year to year basis. Such intra-annual variability is likely to be further reflected in the variability of the upwelling. Changes in the approximated upwelling depth associated with the incident flow speed suggest that when equatorward flow is weak there would be insufficient upwelling to draw up water from deeper than the shelf break [*Allen and Hickey*, 2010], leading to a cessation of upwelling even under an equatorward slope current. This prediction, based on a theoretical calculation (equation (1)), requires further observations or detailed modeling efforts to ascertain how the strength of the slope current influences the strength or even the presence of upwelling through the canyons.

**Acknowledgments**

This study was funded by the UK Natural Environment Research Council project Fluxes Across Sloping Topography of the North East Atlantic (FASTNEt) (NE/I030224/1). M. Porter was funded to visit J.Barth through a SAGES PECRE grant. We thank the crew and scientists of the D376 for the glider and mooring deployments and all involved with nutrient collection as well as glider recoveries and piloting. The data are all available on request from the British Oceanographic Data Centre (http://www.bodc.ac.uk/projects/uk/fastnet/data_inventories/) or through contacting the relevant data manager listed therein.

## References

Alford, M. H., and P. Maccready (2014), Flow and mixing in Juan de Fuca Canyon, Washington, *Geophys. Res. Lett.*, *41*, 1608–1615, doi:10.1002/2013GL058967.

Allen, S., and X. Durrieu de Madron (2009), A review of the role of submarine canyons in deep-ocean exchange with the shelf, *Ocean Sci.*, *5*, 607–620.

Allen, S. E. (2000), *On Subinertial Flow in Submarine Canyons: Effect of Geometry*, Atmos. Sci. Program., University of British Colombia.

Allen, S. E. and B. Hickey (2010), Dynamics of advection-driven upwelling over a shelf break submarine canyon, *J. Geophys. Res.*, *115*, C08018, doi:10.1029/2009JC005731.

Alvarez, A., J. Tintoré, and A. Sabatés (1996), Flow modification and shelf-slope exchange induced by a submarine canyon off the northeast Spanish coast, *J. Geophys. Res.*, *101*, 12,043–12,055.

Barnes, S. L. (1994), Applications of the Barnes objective analysis scheme. Part II: Improving derivative estimates, *J. Atmos. Oceanic Technol.*, *11*, 1449–1458.

Bourillet, J. F., J. Y. Reynaud, A. Baltzer, and S. Zaragosi (2003), The 'Fleuve Manche': The submarine sedimentary features from the outer shelf to the deep-sea fans, *J. Quat. Sci.*, *18*, 261–282.

Brink, K. H. (1998), Deep-sea forcing and exchange processes, in *The Sea, Vol. 10: The Global Coastal Ocean*, edited by K. H. Brink and A. R. Robinson, pp. 151–167, John Wiley and Sons, N. Y.

Canals, M., R. Danovaro, S. Heussner, V. Lykousis, P. Puig, F. Trincardi, A. Calafat, X. Durrieu de Madron, A. Palanques, and A. Sanchez-Vidal (2009), Cascades in Mediterranean submarine grand canyons, *Oceanography*, *22*, 26–43.

Carter, G. S., and M. C. Gregg (2002), Intense, variable mixing near the head of Monterey Submarine Canyon, *J. Phys. Oceanogr.*, *32*, 3145–3165.

Cole, S. T., and D. L. Rudnick (2012), The spatial distribution and annual cycle of upper ocean thermohaline structure, *J. Geophys. Res.*, *117*, C02027, doi:10.1029/2011JC007033.

De Leo, F. C., C. R. Smith, A. A. Rowden, D. A. Bowden, and M. R. Clark (2010), Submarine canyons: Hotspots of benthic biomass and productivity in the deep sea, *Proc. R. Soc. B.*, *277*(1695): 2783–2792.

Duineveld, G., M. Lavaleye, E. Berghuis, and P. De Wilde (2001), Activity and composition of the benthic fauna in the Whittard Canyon and the adjacent continental slope (NE Atlantic), *Oceanol. Acta*, *24*, 69–83.

Freeland, H., and K. Denman (1982), A topographically controlled upwelling center off southern Vancouver Island, *J. Mar. Res.*, *40*, 1069–1093.

Garau, B., S. Ruiz, W. G. Zhang, A. Pascual, E. Heslop, J. Kerfoot, and J. Tintoré (2011), Thermal lag correction on Slocum CTD glider data, *J. Atmos. Oceanic Technol.*, *28*, 1065–1071.

Grasshoff, K., K. Kremling, and M. Ehrhardt (2009), *Methods of Seawater Analysis*, John Wiley, Hoboken, N. J.

Green, J. M., J. H. Simpson, S. Legg, and M. R. Palmer (2008), Internal waves, baroclinic energy fluxes and mixing at the European shelf edge, *Cont. Shelf Res.*, *28*, 937–950.

Gruber, N. (2015), Ocean biogeochemistry: Carbon at the coastal interface, *Nature*, *517*, 148–149.

Hagen, E. (2001), Northwest African upwelling scenario, *Oceanol. Acta*, *24*, 113–128.

Harvey, J. (1982), $\theta$-S relationships and water masses in the eastern North Atlantic, *Deep Sea Res., Part A*, *29*, 1021–1033.

Hopkins, J., J. Sharples, and J. Huthnance (2012), On-shelf transport of slope water lenses within the seasonal pycnocline, *Geophys. Res. Lett.*, *39*, L08604, doi:10.1029/2012GL051388.

Huthnance, J. (1984), Slope currents and "JEBAR," *J. Phys. Oceanogr.*, *14*, 795–810.

Huthnance, J. M., H. Coelho, C. R. Griffiths, P. J. Knight, A. P. Rees, B. Sinha, A. Vangriesheim, M. White, and P. G. Chatwin (2001), Physical structures, advection and mixing in the region of Goban spur, *Deep Sea Res., Part II*, *48*, 2979–3021.

Huthnance, J. M., J. T. Holt, and S. L. Wakelin (2009), Deep ocean exchange with west-European shelf seas, *Ocean Sci.*, *5*, 621–634.

Hydes, D. J., et al. (2001), Supply and demand of nutrients and dissolved organic matter at and across the NW European shelf break in relation to hydrography and biogeochemical activity, *Deep Sea Res., Part II*, *48*, 3023–3047.

Inall, M., D. Aleynik, T. Boyd, M. Palmer, and J. Sharples (2011), Internal tide coherence and decay over a wide shelf sea, *Geophys. Res. Lett.*, *38*, L23607, doi:10.1029/2011GL049943.

Jones, C., E. Creed, S. Glenn, J. Kerfoot, J. Kohut, C. Mudgal, and O. Schofield (2005) Slocum gliders—A component of operational oceanography. in *Proc. 14th Int. Symp. on Unmanned Untethered Submersible Technology*, Lee, NH, Autonomous Undersea Systems Institute.

JNCC (2013), *MCZ Site Summary Document: The Canyons MCZ*, version 4.0, U. K. [Available at jncc.defra.gov.uk/marineprotectedareas.]

Jordi, A., J. Klinck, G. Basterretxea, A. Orfila, and J. Tintoré (2008), Estimation of shelf-slope exchanges induced by frontal instability near submarine canyons, *J. Geophys. Res.*, *113*, C05016, doi:10.1029/2007JC004207.

Klinck, J. M. (1989), Geostrophic adjustment over submarine canyons. *J. Geophys. Res.*, *94*, 6133–6144.

Klymak, J. M., W. Crawford, M. H. Alford, J. A. Mackinnon, and R. Pinkel (2015), Along-isopycnal variability of spice in the North Pacific, *J. Geophys. Res. Oceans*, *120*, 2287–2307, doi:10.1002/2013JC009421.

Kundu, P. K. (1976), Ekman veering observed near the ocean bottom, *J. Phys. Oceanogr.*, *6*, 238–242.

Kunze, E., L. K. Rosenfeld, G. S. Carter, and M. C. Gregg (2002), Internal waves in monterey submarine canyon, *J. Phys. Oceanogr.*, *32*, 1890–1913.

Laruelle, G. G., R. Lauerwald, B. Pfeil, and P. Regnier (2014), Regionalized global budget of the CO2 exchange at the air-water interface in continental shelf seas, *Global Biogeochemi. Cycles*, *28*, 1199–1214, doi:10.1002/2014GB004832.

Munk, W. (1981), Internal waves and small-scale processes, in *Evolution of Physical Oceanography Scientific Surveys in Honor of Henry Stommel*, edited by B. A Warren and C. Wunsch, pp. 264–291, MIT Press.

Pingree, R. and B. Le Cann (1989), Celtic and Armorican slope and shelf residual currents, *Prog. Oceanogr.*, *23*, 303–338.

Pollard, R., M. Grifftths, S. Cunningham, J. Read, F. F. Pérez, and A. F. Ríos (1996), Vivaldi 1991-A study of the formation, circulation and ventilation of Eastern North Atlantic Central Water, *Prog. Oceanogr.*, *37*, 167–192.

Porter, M., M. Inall, J. Green, J. Simpson, A. Dale, and P. Miller (2016), Drifter observations in the summer time bay of Biscay slope current, *J. Mar. Syst.*, *157*, 65–74.

Proctor, R., J. T. Holt, J. I. Allen, and J. Blackford (2003), Nutrient fluxes and budgets for the North West European Shelf from a three-dimensional model, *Sci. Total Environ.*, *314–316*, 769–785.

Rees, A. P., I. Joint, and K. M. Donald (1999), Early spring bloom phytoplankton-nutrient dynamics at the Celtic Sea Shelf Edge, *Deep Sea Res. Part I*, *46*, 483–510.

Rudnick, D. L., R. E. Davis, C. C. Eriksen, D. M. Fratantoni, and M. J. Perry (2004), Underwater gliders for ocean research, *Mar. Technol. Soc. J.*, *38*, 73–84.

Savoye, B., N. Babonneau, B. Dennielou, and M. Bez (2009), Geological overview of the Angola–Congo margin, the Congo deep-sea fan and its submarine valleys, *Deep Sea Res., Part II*, *56*, 2169–2182.

Simpson, J. H. and R. R. McCandliss (2013), ''The Ekman Drain'': A conduit to the deep ocean for shelf material, *Ocean Dyn.*, *63*, 1063–1072.

Simpson, J. H., and J. Sharples (2012), *Introduction to the Physical and Biological Oceanography of Shelf Seas*, Cambridge Univ. Press, Cambridge and N. Y.

Thomas, H., Y. Bozec, K. Elkalay, and H. J. W. De Baar (2004), Enhanced open ocean storage of $CO_2$ from shelf sea pumping, *Science*, *304*, 1005–1008.

Tsunogai, S., S. Watanabe, and T. Sato (1999), Is there a ''continental shelf pump'' for the absorption of atmospheric CO2?, *Tellus, Ser. B*, *51*, 701–712.

Vlasenko, V., N. Stashchuk, M. E. Inall, and J. E. Hopkins (2014), Tidal energy conversion in a global hot spot: On the 3-D dynamics of baroclinic tides at the Celtic Sea shelf break, *J. Geophys. Res. Oceans*, *119*, 3249–3265, doi:10.1002/2013JC009708.

Vlasenko, V., N. Stashchuk, M. E. Inall, M. Porter, and D. Aleynik (2016), Focusing of baroclinic tidal energy in a canyon, *J. Geophys. Res. Oceans*, *121*, 2824–2840, doi:10.1002/2015JC011314.

White, M. (2003), Comparison of near seabed currents at two locations in the Porcupine Sea Bight—Implications for benthic fauna, *J. Mar. Biol. Assoc. U. K.*, *83*, 683–686.

Xu, W., P. I. Miller, G. D. Quartly, and R. D. Pingree (2015), Seasonality and interannual variability of the European Slope Current from 20years of altimeter data compared with in situ measurements, *Remote Sens. Environ.*, *162*, 196–207.